Inorganica Chimica Acta, 190 (1991) 257–264

Rhenium(V) and technetium(V) complexes with *N*-[2(1*H*-pyrolylmethyl)]-*N*′-(4-pentene-3-one-2)ethane-1,2-diaminate ($C_{12}H_{16}N_3O$, MRP 20). X-ray crystal structures of H_3MRP 20 and TcO(MRP 20)

Gillian F. Morgan, Marcel Deblaton, Wasif Hussein, John R. Thornback
MEDGENIX Group, 6220 Fleurus (Belgium)

Guy Evrard, François Durant
Facultés Notre Dame de la Paix, Namur, Department of Chemistry, 5000 Namur (Belgium)

Joachim Stach
University of Leipzig, Department of Chemistry, Talstrasse 35, Leipzig O-7010 (FRG)

Ulrich Abram* and Sonja Abram
Central Institute of Nuclear Research Rossendorf, PF 19, Dresden O-8051 (FRG)

(Received September 3, 1991)

Abstract

Synthesis of *N*-[2(1*H*-pyrolylmethyl)]-*N*′-(4-pentene-3-one-2)ethane-1,2-diamine has been effected and the compound characterised by X-ray diffraction. Crystal data for $C_{12}H_{19}N_3O$: space group $P2_1/c$: $a=10.358(3)$, $b=7.953(1)$, $c=15.640(4)$ Å, $\beta=101.63(1)°$, $V=1261(2)$ Å^3 to give $Z=4$ for $D=1.165$ g cm^{-3}. Structure solution and refinement based on 2114 reflections converged at $R=0.064$, $R_w=0.079$. Reaction of this molecule with $Bu_4N[TcO(ethylene\ glycolate)_2]$ results in the formation of a neutral technetium(V) complex [TcOL]. The X-ray structure of this complex confirms a five-coordinate, square based pyramidal geometry with no crystallographic axes of symmetry. Crystal data: orthorhombic space group $P2_12_12_1$; $a=11.701(1)$, $b=14.949(2)$, $c=7.516(1)$ Å, $V=1314.6$ Å^3 to give $Z=4$ for $D=1.68$ g cm^{-3}. Structure resolution and refinement based on 2115 reflections converged at $R=0.037$, $R_w=0.033$. Reaction of *N*-[2(1*H*-pyrolylmethyl)]-*N*′-(4-pentene-3-one-2)ethane-1,2-diamine with rhenium(V) oxotrichlorobistriphenylphosphine $[ReOCl_3(PPh_3)_2]$ or a rhenium(V) glycolato precursor yields the [ReOL] complex. The compounds have been studied by NMR, UV–Vis, IR spectroscopy as well as by mass spectrometry. The obtained results have been discussed in terms of the complex formation and the different transition metals.

Introduction

There is considerable interest in the chemistry of technetium due to its increased availability and widespread used in diagnostic nuclear medicine. The favourable nuclear properties of the metastable isotope ^{99m}Tc ($E=140$ keV, half-life $t_{1/2}=6.02$ h) allow images of high resolution to be obtained with a low radiation dose to the patient [1]. There is also an increasing interest being shown in rhenium chemistry as isotopes of rhenium, specifically ^{186}Re and ^{188}Re, are potentially useful for radiotherapeutic applications [2].

The ^{99m}Tc complex with *N*-[2(1*H*-pyrolylmethyl)]-*N*′-(4-pentene-3-one-2)ethane-1,2-diamine (**I**, H_3-MRP 20** represents the prototype of a new class of ligands which allow facile derivatisation (see **II**).

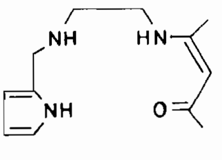

I

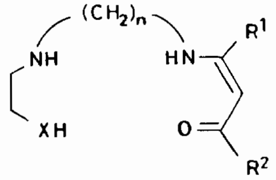

II

This complex is currently being evaluated as a cerebral perfusion tracer and shows promising Phase I/II

---

*Author to whom correspondence should be addressed.

**MRP = Medgenix radiopharmaceutical.

0020-1693/91/$3.50

clinical results [3]. A potential clinical use generates an interest in the chemical structure and the spectroscopical properties of the new agent as well as of its rhenium analog. Milligram scale syntheses and spectroscopic studies on technetium compounds have been done with the long-lived isotope ^{99}Tc (weak β^--emitter, $E_{max}=0.3$ MeV, $t_{1/2}=2.12\times10^5$ years).

Experimental

Health precautions

All work involving ^{99}Tc was done in laboratories approved for the use of low levels of radioactive materials. Use of milligram quantities of ^{99}Tc does not present a health hazard since common laboratory materials provide adequate shielding. Bremsstrahlung is not a significant problem with small quantities due to the low energy of the beta particle emission, but normal radiation safety procedures must be used at all times to prevent contamination.

Syntheses

H_3MRP 20 (I)

9.5 g (0.1 mol) pyrrole-2-aldehyde in 80 ml dry acetonitrile were slowly added to 0.6 mol ethane-1,2-diamine. The reaction was stirred overnight in the presence of 4 Å molecular sieves and filtered, then evaporated to dryness under vacuum. The residue was dissolved in 100 ml methanol in an ice bath and 0.1 mol sodium borohydride was slowly added with stirring. After 2 h, the methanol was removed by vacuum and 100 ml water was added. After addition of 20 g potassium hydroxide, the mixture was extracted with 5×5 ml dichloromethane. After combining the organic phases and drying over anhydrous potassium carbonate, the solvent was evaporated yielding a yellow oil which mainly consists of *N*-[2(1-H-pyrolylmethyl)]ethane-1,2-diamine. 1.4 g of this crude product in 10 ml acetonitrile was mixed with 2 ml (0.02 mol) pentan-2,4-dione in 10 ml acetonitrile. After stirring for 3 h, the solvent was evaporated and the residue extracted with dichloromethane. The resulting yellow oil was purified on silica with a gradient of methanol in ethyl acetate/0.5% diethylamine as eluant to give a pale yellow oil that solidified upon cooling at 4 °C. The final product was recrystallised from diisopropylether to give fine needle-like crystals. Yield 65%. Melting point 75 °C. *Anal.* Found: C, 65.01; H, 8.73; N, 18.88. Calc. for $C_{12}H_{19}N_3O$: C, 65.12; H, 8.65; N, 18.99%. IR: N–H 3352 cm^{-1}, C=O 1598 cm^{-1}.

^{1}H NMR: 1.6 s (1H, NH); 1.9 s (3H, CH_3); 2.05 s (3H, CH_3); 2.83 t (2H, CH_2); 3.29 qu (2H, CH_2); 3.82 s (2H, pyrrole-CH_2) 5.0 s (1H, CH); 5.98 qu (1H, pyrrole); 6.08, 6.75 2 qu (1H, pyrrole); 9.6, 11.22 2 s (2H, NH) ppm. ^{13}C NMR: $\delta=19.0$; 28.6; 42.6; 46.1; 47.3; 95.4; 105.98; 107.4; 117.6; 130.3; 162.7; 194.7 ppm.

TcO(MRP 20)

50 mg (0.1 mmol) $(Bu_4N)TcOCl_4$ was dissolved in a minimum amount of methanol to which 2 ml ethylene glycol was added with stirring. To the resulting green solution, solid sodium acetate was added until a deep-purple coloration was sustained. 25 mg (0.13 mmol) H_3MRP 20 in methanol was added with stirring. After 1 h, the yellow–brown precipitate formed was collected by suction filtration and recrystallised from a chloroform/isopropanol mixture to give orange–red needles. Yield 73% (based on Tc). *Anal.* Found: C, 43.1; H, 5.1; N, 12.4; Tc, 30.0. Calc. for $TcC_{12}H_{16}N_3O_2$: C, 42.2; H, 4.8; N, 12.6; Tc, 29.7%. IR: Tc=O 953 cm^{-1}. UV–Vis ($\lambda_{max}(\lg\epsilon)$): 255 (4.02); 301 (3.82); 343 (3.84). ^{1}H NMR: 2.23 s (3H, CH_3); 2.25 s (3H, CH_3); 3.92 m (1H, CH_2); 4.15 m (1H, CH_2); 4.30 m (1H, CH_2); 4.39 m (1H, CH_2); 4.54 AB ($J_{AB}=16$ Hz) (1H, pyrrole-CH_2); 5.30 AB ($J_{AB}=16$ Hz) (1H, pyrrole-CH_2); 5.43 s (1H, CH); 6.08 d of d (1H, pyrrole); 6.35 t (1H, pyrrole); 7.35 d of d (1H, pyrrole) ppm. ^{13}C NMR: $\delta=22.9$; 26.1; 59.1; 64.8; 66.8; 100.7; 103.0; 110.8; 123.8; 146.2; 171.3; 186.0 ppm.

ReO(MRP 20)

(a) 500 mg (0.88 mmol) $[ReOCl_3(Ph_3P)_2]$ was added to a solution of 190 mg (1 mmol) H_3MRP 20 and 300 mg triethylamine in dry ethanol and stirred at 65–70 °C for 5.5 h. The resulting bright red solution was left at room temperature for 44 h. A red–brown crystalline solid separated which was collected and washed with ethanol. The solid was dissolved in dichloromethane and filtered. Upon addition of ethanol and concentration of the solvent, a red–brown microcrystalline solid was collected by filtration and washed successively with ethanol and pentane and dried *in vacuo* at 4 °C for 2 h. Yield 32% (based on Re).

(b) In a similar manner to the technetium preparation [4], the rhenium glycolate anion was prepared *in situ* from 77 mg (0.1 mmol) $(Bu_4N)ReOBr_4$ [5]. 30 mg (0.136 mmol) H_3MRP 20 in methanol was added and stirred at room temperature for 10 h. The resulting deep brown solution was kept overnight at 4 °C. During this time a brown solid formed which was filtered and washed with ethanol. Yield 25% (based on Re). *Anal.* Found: C, 34.3; H, 3.9; N, 9.70. Calc. for $ReC_{12}H_{16}N_3O_2$: C, 34.3; H, 3.8; N, 9.99. IR: Re=O 963 cm^{-1}, UV–Vis ($\lambda_{max}(\lg\epsilon)$): 235

(4.06), 323 (3.77). ^{1}H NMR: 2.35 s (3H, CH_3); 2.43 s (3H, CH_3); 3.95 m (1H, CH_2); 4.15 m (1H, CH_2); 4.34 m (1H, CH_2); 4.64 m (1H, CH_2); 4.35 AB ($J_{AB} = 17$ Hz) (1H, pyrrole-CH_2); 5.42 AB ($J_{AB} = 17$ Hz) (1H, pyrrole-CH_2); 5.55 s (1H, CH); 6.25 d of d (1H-pyrrole); 6.44 t (1H-pyrrole); 7.40 d (1H pyrrole) ppm.

Measurements

Routine IR spectra were recorded as KBr discs on a UR 20 (Carl Zeiss Jena) and Perkin-Elmer 1600 series FT-IR spectrophotometer. ^{1}H NMR and ^{13}C NMR spectra were obtained in chloroform solution on a Bruker AM-250 spectrometer with a TMS standard. Fast-atom-bombardment mass spectra and electron impact mass spectra were recorded on a VG ZAB HSQ spectrometer. FAB spectra measurements were performed in a glycerol matrix; argon was used as a primary beam gas. The ion gun was operated at 8 kV and 100 μA. For the measurement of the electron impact mass spectra, standard conditions were used. Elemental analysis was performed by G. D. Searle, Belgium and the Microanalytical Services, School of Chemistry, University of Birmingham, UK. The technetium content was determined by Bremsstrahlung measurements with a well-type Na(Tl)I-scintillator according to a standard procedure [6].

X-ray diffraction

X-ray data were collected at room temperature on an Enraf-Nonius CAD4 diffractometer. Crystal data and details of the refinement are summarised in Table 1.

H_3MRP 20

A colourless prismatic crystal was used. A total of 3616 reflections ($-12 \leq h \leq 12$, $-8 \leq k \leq 9$, $0 \leq l \leq 19$) was collected in the range $4 \leq 2\theta \leq 144°$, of which 2474 were unique reflections ($R_{int} = 0.026$) with 2114 having $I > 2\sigma(I_o)$ being used in the refinement. No absorption correction was applied. The structure was solved by direct methods (SHELXS 86 [7]) and refined by full-matrix least-squares techniques using the SHELX-76 [8] crystallographic package to a final $R = 0.064$ and $R_w = 0.079$ ($w = 1/\sigma^2F + 0.003F^2$), $S = 1.95$ for 193 variables and 2114 observations.

All hydrogen atoms were found in a difference-Fourier map and assigned isotropic thermal parameters (U) equal to the U_{eq} value of the carrier atom $+0.01$. Their coordinates were refined in the final least-squares cycles. The maximum shift/e.s.d. in the last least-squares cycle was -0.318 (Y/b of C(5)). The final difference-Fourier map had $-0.38 \leq \varphi \leq 0.23$ e Å^{-3}. Table 2 contains selected bond lengths of the non-coordinated ligand.

TABLE 1. Crystal data and refinement parameters for H_3MRP 20 and TcO(MRP 20)

	H_3MRP 20	TcO(MRP 20)
Formula	$C_{12}H_{19}N_3O$	$TcO(C_{12}H_{16}N_3O)$
M_r	221.2	333.2
Crystal dimensions (mm)	0.42×0.25×0.23	0.38×0.15×0.13
Color/form	colorless/prismatic	red–brown/prismatic
Radiation source (Cu Kα graphite-monochromated)	$\lambda = 1.54178$ Å	$\lambda = 1.54178$ Å
μ (cm^{-1})	5.33	84.59
Space group	monoclinic, $P2_1/c$	orthorhombic, $P2_12_12_1$
Cell parameters		
a (Å)	10.358(3)	11.701(1)
b (Å)	7.953(1)	14.949(2)
c (Å)	15.640(4)	7.516(1)
α (°)	90	90
β (°)	101.63(1)	90
γ (°)	90	90
V (Å^3)	1261(2)	1314.6(2)
Z	4	4
φ_{calc} (g/cm)	1.165	1.679
R, R_w	0.064, 0.079	0.027, 0.033
Temperature (K)	293	293
No. reflections measured		
Total	3616	2433
Used in refinement	2114	2120

TABLE 2. Bond lengths (Å) in H_3MRP 20 (for the numbering of the atoms see Fig. 1)

O(1)–C(2)	1.257(2)	C(9)–N(10)	1.429(3)
C(2)–C(3)	1.501(2)	N(10)–C(11)	1.451(3)
C(2)–C(4)	1.404(3)	C(11)–C(12)	1.496(2)
C(4)–C(5)	1.396(2)	C(12)–N(13)	1.356(2)
C(5)–C(6)	1.505(3)	N(13)–C(14)	1.372(2)
C(5)–N(7)	1.313(2)	C(14)–C(15)	1.347(3)
N(7)–C(8)	1.462(2)	C(15)–C(16)	1.408(2)
C(8)–C(9)	1.537(3)	C(16)–C(12)	1.379(2)

TABLE 3. Selected bond lengths and angles for TcO(MRP 20)

Bond lengths (Å)			
Tc–O(1)	1.666(3)	C(4)–C(5)	1.409(4)
Tc–N(6)	2.033(4)	C(5)–C(8)	1.533(4)
Tc–N(14)	1.993(4)	C(5)–N(6)	1.343(4)
Tc–O(2)	2.025(3)	N(6)–C(9)	1.468(4)
Tc–N(11)	1.897(4)	C(9)–C(10)	1.503(4)
O(2)–C(3)	1.292(3)	C(10)–N(11)	1.459(4)
C(3)–C(4)	1.336(4)	N(11)–C(12)	1.469(4)
C(3)–C(7)	1.504(4)	C(12)–C(13)	1.485(4)
Bond angles (°)			
O(1)–Tc–O(2)	112.3(1)	O(1)–Tc–N(14)	110.9(2)
O(1)–Tc–N(6)	108.7(2)	O(1)–Tc–N(11)	109.8(1)
O(2)–Tc–N(14)	83.7(2)	O(2)–Tc–N(6)	87.9(1)
O(2)–Tc–N(11)	137.8(1)	N(6)–Tc–N(11)	80.7(1)
N(11)–Tc–N(14)	79.5(2)	N(6)–Tc–N(14)	139.7(2)
Tc–O(2)–C(3)	126.6(3)		

TcO($C_{12}H_{16}N_3O$)

A dark red–brown prismatic crystal which was suitable for X-ray diffraction was obtained by slow evaporation of a $CHCl_3$/isopropanol solution. A total of 2433 reflections ($0 \leqslant h \leqslant 14$, $-15 \leqslant k \leqslant 18$, $0 \leqslant l \leqslant 9$) was collected in the range $4 \leqslant 2\theta \leqslant 144$, of which 2137 were unique reflections ($R_{\text{int}} = 0.027$) with 2120 having $I > 2.5\sigma(I_o)$ being used in the refinement. The structure was solved by Patterson (SHELXS-86) and refined by full-matrix least-squares techniques (NRCVAX [9]) to a final $R = 0.027$ and $R_w = 0.033$ ($w = 1/\sigma^2F + 0.002F^2$), $S = 1.47$ for 163 variables and 2120 observations. Numerical absorption correction was applied. Thirteen hydrogen atoms were found in a difference-Fourier map, the remaining three were calculated; their coordinates were not refined. The maximum shift/e.s.d. in the last least-squares cycle was 0.357 (Z/c of C(8)). The final difference-Fourier map had $-1.45 \leqslant \varphi \leqslant 0.36$ e Å^{-3}.

Selected bond distances and angles are given in Table 3. All calculations were performed either on the IBM 9377 computer of the SCF (Namur) or the Microvax II of our laboratory. Atomic scattering factors are from SHELX-76 or NRCVAX. The absolute structure was not determined.

Results and discussion

The chemistry of neutral technetium(V) oxo compounds has been extensively studied since it was shown that several of these complexes have the ability to cross the blood–brain barrier [10–12]. With quadridentate ligands having N_4, N_2S_2 or N_3S donor sets, five-coordinate square pyramidal [TcOL] complexes are formed; six-coordinate complexes are formed from quadridentate symmetrical Schiff bases with a halide or water *trans* to the yl oxygen [13]. We have developed a new series of potentially quadridentate N_3O ligands with the ability to lose three protons upon coordination. These asymmetric ligands are easily synthesised from readily available reagents and the synthetic pathway allows facile derivatisation. The title ligand, the prototype of the series, was found to react readily with ^{99m}Tc and subsequent biological studies in animals and man showed it has potential as a tracer for regional cerebral blood flow (rCBF). The biological findings of the no-carrier added chemistry are presented elsewhere [14]. As the prototype of a ligand series with good potential in nuclear medicine, a full X-ray structure determination was carried out to unequivocally characterise it. The ORTEP is shown in Fig. 1. The full structural and spectroscopic characterisation of the ligand enables us to discuss differences which are caused by the formation of the chelate rings during the complex formation.

The reaction of H_3MRP 20 with $(Bu_4N)TcOCl_4$ which is a common starting material for the synthesis of oxotechnetium(V) complexes does not lead to the desired monomeric product, but yields a black–brown oligomeric powder. FAB mass spectrometry suggests TcL_3 subunits without evidence for a Tc=O core. A monomeric product can be obtained using the well established Tc(V) precursor $[TcO(eg)_2]^-$, which can be easily prepared from $TcOCl_4^-$ by subsequent addition of ethylene glycol and sodium acetate [4]. The purple solution immediately reacts *in situ* with the title ligand yielding a yellow–brown compound that spontaneously precipitates from the mother liquor and recrystallises from $CHCl_3$/isopropanol to give orange–red needles. The IR spectrum of the

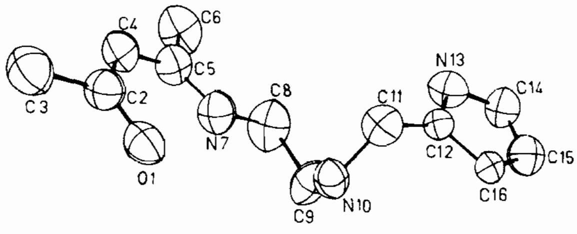

Fig. 1. ORTEP drawing of H_3MRP 20 along with the atomic numbering scheme.

compound shows a strong absorption at 953 cm^{-1}, which is in the characteristic range for the Tc=O mono-oxo core, 920–1020 cm^{-1}. Strong absorptions at 1580 and 1524 cm^{-1} are assigned to the C=N azomethine and the C=O stretches. The ^1H NMR spectrum shows a series of multiplets at 4.39, 4.30, 4.15 and 3.92 ppm from the CH_2 protons of the ethane-1,2-diamine backbone which resonate as four distinct signals due to the asymmetry of the ligand and non-equivalence of each ^1H environment. Due to the square pyramidal oxo technetium core the CH_2 protons neighbouring the pyrrole ring are diastereotopic and appear as an AB type quartet with a geminal coupling constant of $J_{AB} = 16$ Hz. The general downfield shift of the proton NMR signals with respect to their positions in the spectrum of the free ligand is a consequence of the formation of the chelate rings and reflects some double bond character for all bonds in the backbone of the ligand which is common for transition metal complexes with Schiff bases. This effect is confirmed by the results of the X-ray crystal structure (*vide infra*). The pyrrole protons are split into a triplet and two doublet of doublets at 6.08, 6.35 and 7.35 ppm. Additionally, the signal at 6.08 ppm shows some evidence of coupling with the CH_2 protons adjacent to the pyrrole ring. The three NH protons, seen in the ^1H spectrum of the free ligand at 11.2, 9.6 and 1.6 ppm, are not observed confirming the triple deprotonation of the ligand upon coordination with technetium. The $^{13}C\{^1H\}$ spectrum is consistent with the structure of the complex. The ^{99}Tc NMR resonance was not observed, but given the low symmetry of the molecule this was to be expected [15]. The electron impact (EI) mass spectrum (Fig. 2(a)) shows an intense signal at $m/z = 333$, which represents the molecular ion. Further metal-containing fragments are of lesser intensity and more information was derived from the MIKE (mass analysed ion kinetic energy) spectrum obtained by mass selection of the molecular ions. The metastable decomposition of the mass selected ions yields a large number of daughter ions shown in Fig. 2(b). The oxygen of the Tc=O group is lost in the fragmentation process. This compares well to the mass spectral fragmentation of other oxo technetium complexes [16] and contrasts their behaviour with Tc(V) complexes containing a Tc≡N nitrido core [17]. The complex shows equal tendency to fragment at both the pyrrole and the Schiff base parts of the structure. A similar pattern was observed in the ligand, where a strong signal for the molecular ion at $m/z = 221$ is found. Table 4 summarises the fragmentation patterns of H_3MRP 20, TcO(MRP 20) and ReO(MRP 20). The extraction of H_2O and $CH_2{=}CH_2$ ($[M-18]^+$ and $[M-28]^+$) are not immediately obvious from the complex structure, however this disintegration pattern is observed in both the technetium and rhenium complexes and has also been seen with similar technetium compounds in our laboratories [18, 19]. The two fragments are not identified in the ligand spectrum and this suggests the formation of an intermediate such as that shown in Fig. 3. Such a fragmentation pattern would only be possible with metal present to stabilise the rest of the molecule.

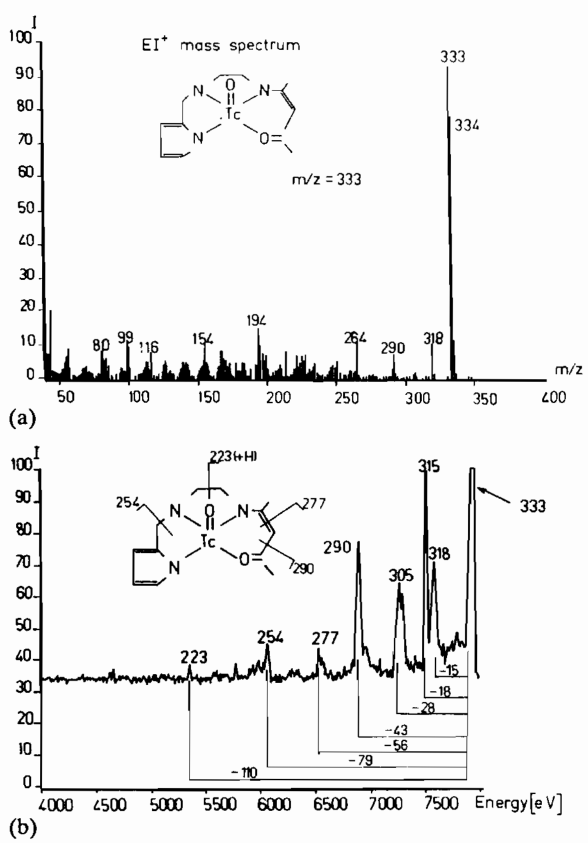

Fig. 2. (a) EI⁺ mass spectrum of TcO(MRP 20), showing the molecular ion at $m/z = 333$; (b) MIKE (mass analyzed ion kinetic energy) spectrum indicating the fragmentation pattern of the base peak.

A single crystal X-ray structural determination was undertaken to confirm the postulated five-coordinate technetium(V) square planar configuration. The ORTEP is given in Fig. 4. The structure represents a slightly distorted square based pyramid with the technetium lying out of the ligand plane and the pyrrole group also directed up out of the plane of the molecule towards the technetium–oxo core. The Tc=O bond length of 1.670 Å is comparable to other quadridentate, square pyramidal technetium(V) complexes [20]. The bond lengths which are given in Table 3 confirm some double bond character for all bonds in the chelate ligand. A comparison

TABLE 4. Selected characteristic fragments of the MS decay for H_3MRP 20, TcO(MRP 20) and ReO(MRP 20)

Abstracted group	m/z		
	H_3MRP 20	TcO(MRP 20)	ReO(MRP 20)[a]
CH_3	206	318	406
H_2O		315	403
CH_2–CH_2		305	393
CH_3, CH_3			391
CH_3CO	178	290	378
CH_3COCH		277	
$CH_3COCHC(CH_3)N$	123		
C_4H_3N			356
$C_4H_3NCH_2$		254	
$C_4H_3NCH_2NH$	127(+H)		
$C_4H_3NCH_2NHCH_2$	113	223	
$C_4H_3NCH_2NH(CH_2)_2$	98		

[a] For ^{187}Re.

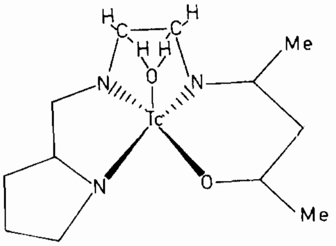

Fig. 3. Structure of the postulated intermediate which leads to the abstraction of H_2O during the mass spectrometric fragmentation of the MO(MRP 20) complexes (M = Tc, Re).

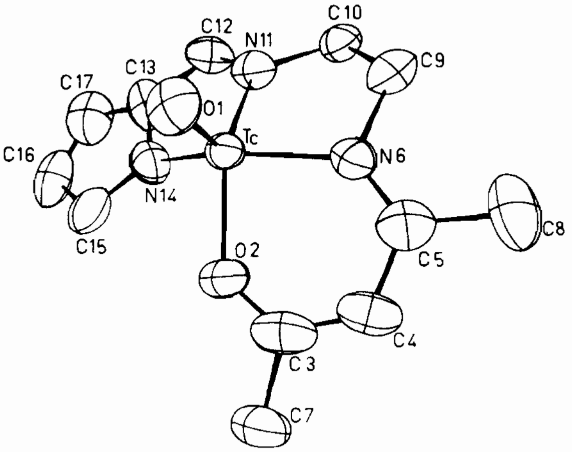

Fig. 4. ORTEP drawing of TcO(MRP 20) along with the atomic numbering scheme.

with the values for the non-coordinated ligand (Table 2) shows that the complex formation leads to a visible lengthening of the C–N and C=O bonds and a shortening of the C–C distances indicating an extended π-electron system.

Previously, only one pyrrole containing technetium complex has been structurally characterized, the binuclear $[(Tc(CO)_3)_2TPP]$, where TPP is *meso*-tetraphenylporphyrin. In this compound the technetium atom is situated above and below the plane of the four pyrrole nitrogen atoms [21]. This is reflected in the weak bonding between Tc–N with an average bond length of 2.32 Å. The Tc–N bond length in TcO(MRP 20) of 1.999 Å is the first communication of its class. It compares very favourably with the reported metal–chelate ring nitrogen bond lengths of 2.047 and 2.032 Å in $[Mo(NO)\{HB(Me_2pz)_3(pyr)_2]$ [22] and 2.11 Å in $[\{\eta\text{-}C_4(CH_3)_2H_2N\}Mn(CO)_3]$ [23].

For the non-symmetric TcO(MRP 20) two distinct Tc–N bond distances were obtained for the ethylene diamine backbond. The longer, weaker bond (2.027 Å) is found between the technetium and azomethine nitrogen and is comparable to the reported value for single bond character (2.166 Å in $[TcO_2(en)_2]^+$ [24] and 2.125 Å in $[TcO_2(cyclam)]^+$ [25] and the average Tc–N oxime bond lengths in PnAO and HM-PAO complexes of 2.087), whereas the Tc–N bond of the deprotonated imino nitrogen (1.894 Å) [26] demonstrates some multiple bond character.

A symmetric Schiff base condensation of ethane-1,2-diamine would result in the ligand *N*,*N*′-ethylenebis(acetylacetone imine), and N_2O_2 system. This reacts with technetium to give a six-coordinate technetium(V) cation, with H_2O occupying the sixth position *trans* to the oxo oxygen [13a]. Since the presence of a ligand in the sixth coordination position is thought to be related to the electronic nature of the *cis* substituents [27] it can be assumed that the additional loss of a proton from the pyrrole N-H is sufficient to stabilise the title complex in five coordination.

The rhenium compound ReO(MRP 20) can be prepared in a similar manner to the technetium complex via an intermediate ethylene glycolato complex or in higher yield from the $[ReOCl_3(Ph_3P)_2]$ precursor. The reaction with $[ReOX_4]^-$ complexes (X = Cl, Br) gives oligomeric products in analogy to the reaction with $[TcOCl_4]^-$, suggesting that the formation of the quadridentate chelate occurs at a slower rate than competing reactions and these latter are preferred when starting with the highly reactive halide complexes. Less reactive starting materials yield the [MOL] chelates in satisfactory yields. The rhenium compound shows the expected Re=O stretching vibration in the IR spectrum at 963 cm^{-1} and a similar proton NMR spectrum to the technetium analogue. The slight differences to the technetium compound which have been found in the chemical shifts and the coupling patterns of the signals cannot be used to derive differences in the bonding properties of the complexes. The EI^+ mass spectrum is characterised by intense peaks at $m/z = 419$ and 421 corresponding to the $^{185}Re/^{187}Re$ isotope pattern of the molecular ion and peaks at $[M^+ - 1]$. Main fragments derived from the MIKE spectra of the mass selected ions of the peak $m/z = 421$ are listed in Table 4. The rhenium complex is considerably less stable in solution than its technetium analogue, decomposing readily. This may be due to a reaction in the sixth position *trans* to the M=O bond and following solvolysis. Similar reactions can also be observed in Tc complexes with similar ligands which carry ethyl groups in R^1 and R^2 positions (see **II**). Spectroscopic studies to explain these decomposition reactions are in progress.

Supplementary material

Atom coordinates, anisotropic thermal parameters and calculated and observed structure factors are available from author G.E. (University of Namur) on request.

Acknowledgements

The authors thank Mr Mbonimana of the University of Marburg for his technical assistance with the measurement of the NMR spectra. We also acknowledge the National Belgian Foundation for Scientific Research (F.R.N.S.), I.B.M. Belgium and the Facultés Universitaires Note Dame de la Paix (F.N.D.P.) for the use of the Namur Scientific Computing Facility.

References

1 M. J. Clarke and L. Podbielski, *Coord. Chem. Rev., 78* (1987) 253.

2 E. Deutsch, K. Libson, J. L. Vanderheyden, A. R. Ketring and H. R. Maxon, *Nucl. Med. Biol., 113* (1986) 465.

3 A. Bossuyt, G. F. Morgan, M. Deblaton, R. Pirotte, A. Chirico, P. Clemens, P. van den Broeck and J. R. Thornback, *J. Nucl. Med., 32* (1991) 399.

4 A. Davison, B. V. DePamphilis, A. G. Jones, K. J. Franklin and C. J. L. Lock, *Inorg. Chim. Acta, 128* (1987) 161.

5 F. A. Cotton and S. J. Lippard, *Inorg. Chem., 4* (1965) 1621.

6 R. Münze and B. Grossmann, *Int. J. Appl. Radiat. Isot., 35* (1984) 1073.

7 G. M. Sheldrick, *SHELXS-86*, a programme for the solution of crystal structures, Institut für Anorganische Chemie der Universität, Göttingen, FRG, 1986.

8 G. M. Sheldrick, *SHELX-76*, a programme for crystal structure determination, University of Cambridge, UK, 1976.

9 E. J. Gabe, Y. Le Page, J. P. Charland and F. L. Lee, *J. Appl. Crystallogr., 22* (1989) 384.

10 R. D. Neirinckx, L. R. Canning, I. M. Piper, D. P. Nowotnik, R. D. Pickett, R. A. Holmes, W. A. Volkert, A. M. Forster, P. S. Weiser, J. A. Marriott and S. B. Chaplin, *J. Nucl. Med., 28* (1987) 191.

11 R. C. Walovitch, T. C. Hill, S. T. Garrity, E. H. Cheesman, B. A. Burgess, D. H. O'Leary, A. D. Watson, M. V. Ganey, R. A. Morgan and S. J. Holmes, *J. Nucl. Med., 30* (1989) 1892.

12 H. F. Kung, Y. H. Guo, C. C. Yu, J. Billings, V. Subramaniam and J. Calbrese, *J. Med. Chem., 32* (1989) 433.

13 (a) S. Jurisson, L. F. Lindoy, K. P. Dancey, M. McPartlin, P. A. Tasker, D. K. Uppal and E. Deutsch, *Inorg. Chem., 23* (1984) 227; (b) G. Bandoli, M. Nicolini, U. Mazzi and F. Refosco, *J. Chem. Soc., Dalton Trans.,* (1984) 2505.

14 G. F. Morgan, M. Deblaton, P. Clemens, P. van den Broeck, A. Bossuyt and J. R. Thornback, *J. Nucl. Med., 32* (1991) 500.

15 L. A. O'Connell, R. M. Pearlstein, A. Davison, J. R. Thornback, J. F. Kronauge and A. G. Jones, *Inorg. Chim. Acta, 161* (1989) 39.

16 U. Abram, R. Münze, J. Hartung, L. Beyer, R. Kirmse, K. Köhler, J. Stach, H. Behm and P. T. Beurskens, *Inorg. Chem., 28* (1989) 834.

17 J. Stach and U. Abram, in M. Nicolini, G. Bandoli and U. Mazzi (eds.), *Technetium and Rhenium in Chemistry and Nuclear Medicine 3,* Cortina International, Verona, 1990, pp. 79.

18 U. Abram, S. Abram, G. F. Morgan, J. R. Thornback, M. Deblaton and J. Stach, *Z. Naturforsch., Teil B, 46* (1991) 453.

19 U. Abram, S. Abram, J. Stach, R. Wollert, G. F. Morgan, J. R. Thornback and M. Deblaton, *Z. Anorg. All. Chem., 600* (1991) 15.

20 M. Melnik and J. E. van Lier, *Coord. Chem. Rev., 77* (1987) 275.

21 A. Packard, *8th Int. Symp. Radiopharmaceutical Chemistry, Princeton, NJ, 1990,* Abstr. no. 14.

22 M. Tsutsui, C. P. Houng, D. Ostfeld, T. S. Srivastava, D. L. Cullen and E. F. Meyer, Jr., *J. Am. Chem. Soc., 97* (1975) 3952.

23 N. Al Obaida, A. J. Edwards, C. J. Jones, J. A. McCleverty, B. D. Neaves, F. E. Mabbs and D. Collison, *J. Chem. Soc., Dalton Trans.,* (1989) 127.

24 M. E. Kastner, M. J. Lindsay and M. J. Clarke, *Inorg. Chem., 21* (1982) 2037.

25 S. A. Zuckman, G. M. Freeman, D. E. Troutner, W. A. Volkert, R. A. Holmes, D. G. van der Veer and E. K. Barefield, *Inorg. Chem., 20* (1981) 2386.

26 E. O. Schlemper, D. E. Troutner, L. R. Canning, D. P. Novotnik and R. D. Neirinckx, *Inorg. Chem., 25* (1988) 543.

27 A. Davison and A. G. Jones, *Int. J. Appl. Radiat. Isot., 33* (1982) 875.